



Contents lists available at ScienceDirect

# Bioorganic & Medicinal Chemistry Letters

journal homepage: [www.elsevier.com/locate/bmcl](http://www.elsevier.com/locate/bmcl)



## Discovery of orally bioavailable imidazo[1,2-*a*]pyrazine-based Aurora kinase inhibitors

David B. Belanger<sup>a,\*</sup>, Michael J. Williams<sup>a</sup>, Patrick J. Curran<sup>a</sup>, Amit K. Mandal<sup>a</sup>, Zhaoyang Meng<sup>a</sup>, Matthew P. Rainka<sup>d</sup>, Tao Yu<sup>b</sup>, Neng-Yang Shih<sup>a</sup>, M. Arshad Siddiqui<sup>a</sup>, Ming Liu<sup>c</sup>, Seema Tevar<sup>c</sup>, Suining Lee<sup>c</sup>, Lianzhu Liang<sup>c</sup>, Kimberly Gray<sup>c</sup>, Bohdan Yaremko<sup>c</sup>, Jennifer Jones<sup>c</sup>, Elizabeth B. Smith<sup>c</sup>, Dan B. Prelusky<sup>c</sup>, Andrea D. Basso<sup>c</sup>

<sup>a</sup> Department of Medicinal Chemistry, Merck Research Laboratories, 320 Bent Street, Cambridge, MA 02141, USA

<sup>b</sup> Department of Medicinal Chemistry, Merck Research Laboratories, 2015 Galloping Hill Road, Kenilworth, NJ 07033, USA

<sup>c</sup> Department of Oncology, Merck Research Laboratories, 2015 Galloping Hill Road, Kenilworth, NJ 07033, USA

<sup>d</sup> AMRI, 26 Corporate Circle, PO Box 15098, Albany, NY 12212, USA

### ARTICLE INFO

#### Article history:

Received 30 July 2010

Revised 26 August 2010

Accepted 27 August 2010

Available online 18 September 2010

#### Keywords:

Aurora kinase inhibitors

Imidazo[1,2-*a*]pyrazine

Oral bioavailability

Tumor xenograft mouse model

### ABSTRACT

We report a series of potent imidazo[1,2-*a*]pyrazine-based Aurora kinase inhibitors. Optimization of the solvent accessible 8-position led to improvements in both oral bioavailability and off-target kinase inhibition. Compound **25** demonstrates anti-tumor activity in an A2780 ovarian tumor xenograft model.

© 2010 Elsevier Ltd. All rights reserved.

Aurora kinases (Aurora A, B, and C) are cell cycle regulated serine/threonine kinases expressed only during mitosis.<sup>1</sup> Ubiquitously expressed Aurora A regulates cell cycle events such as centromere maturation, bipolar spindle assembly, mitotic entry and exit, as well as, kinetochore-spindle attachment.<sup>1</sup> Aurora B phosphorylates histone H3, regulates chromosomal remodeling, kinetochore-spindle attachment, and cytokinesis.<sup>1</sup> Aurora C is believed to have a function related to Aurora B but has limited expression.<sup>1</sup> Aurora A and B are essential protein kinases and as such are required for the successful mitotic progression. Depletion of Aurora A by siRNA or small molecule inhibition results in G2/M delay followed by apoptotic cell death, while depletion of Aurora B by siRNA or small molecule inhibition causes aberrant endoreduplication (polyploidy) followed by apoptosis. Abrogation of both Aurora A/B displays an Aurora B siRNA phenotype.<sup>1</sup> Amplification or over expression of Aurora kinases has been observed in multiple tumor types<sup>2–4</sup> and is often correlated with poor prognosis.<sup>5</sup> These data suggest that Aurora kinase inhibitors could be a useful means for treating cancer.

Many Aurora inhibitors (selective Aurora A, selective Aurora B or dual Aurora A/B inhibitors) are currently in Phase I/II trials with several other inhibitors in preclinical development.<sup>4,6</sup> Previously, we

reported the discovery of imidazo[1,2-*a*]pyrazine-based Aurora A/B kinase inhibitors **1** and **2** (Fig. 1).<sup>7</sup> This effort established that the C-3 pyrazole and the C-8 aminoisothiazole groups were essential for good Aurora A/B potency. Additionally, it was determined that small C-6 hydrophobic groups were preferred (e.g., 6-Me, 6-SMe). Subsequent optimization of the solvent accessible 8-position identified compound **3** as a sub-nanomolar, injectable Aurora A/B inhibitor.<sup>8</sup> Importantly, inhibitor **3** demonstrated mechanism-based cell activity and dose dependent anti-tumor activity as single agent or in combination with anti-mitotics such as taxanes and KSP inhibitors.<sup>8,9</sup>

Despite promising in vivo efficacy and an acceptable safety profile, Aurora kinase inhibitor **3** had some potential issues. First, compound **3** exhibited multi-target kinase inhibition extending broadly across the kinome. For example, compound **3** displayed potent Aurora kinase (AGC group) inhibition and cross reactivity with LCK (IC<sub>50</sub> ≤ 1 nM, Tyrosine Kinase group, src family), IRAK4 (IC<sub>50</sub> = 8 nM, Tyrosine Kinase-like group, IRAK family), VEGFR2 (IC<sub>50</sub> ≤ 1 nM, Tyrosine Kinase group, receptor tyrosine kinase family) and CHK1 (IC<sub>50</sub> = 13 nM, CAMK group, CSK family). Indeed, a more extensive evaluation of compound **3** revealed potent inhibition (IC<sub>50</sub> < 20 nM) of the entire src family (data not shown).<sup>10</sup> Second, compound **3** was designed for intravenous dosing and therefore did not show oral bioavailability due to poor absorption and high first pass

\* Corresponding author. Tel.: +1 617 499 3504; fax: +1 617 499 3535.

E-mail address: [david.belanger@merck.com](mailto:david.belanger@merck.com) (D.B. Belanger).

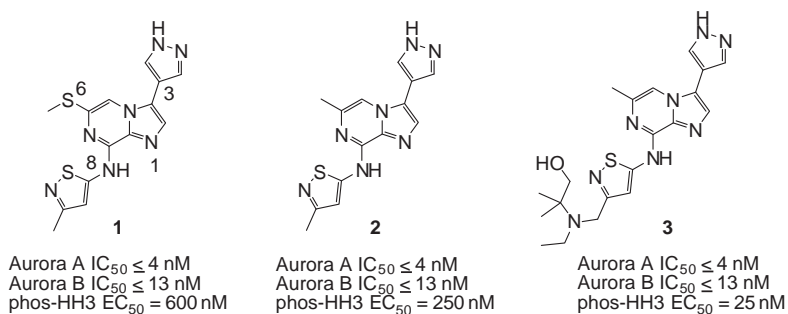
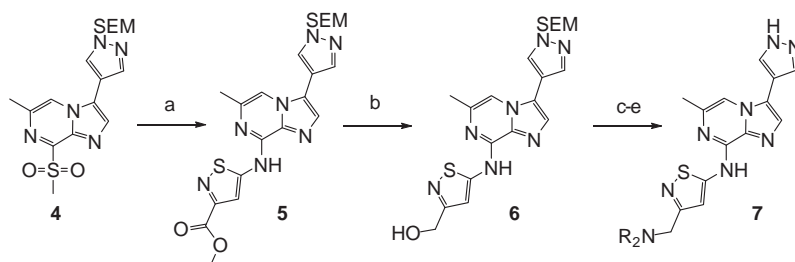
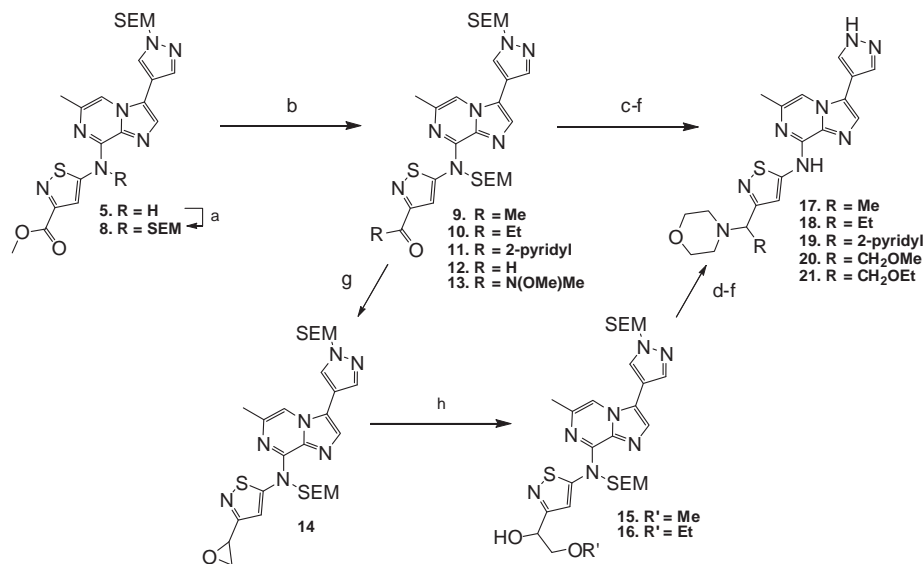


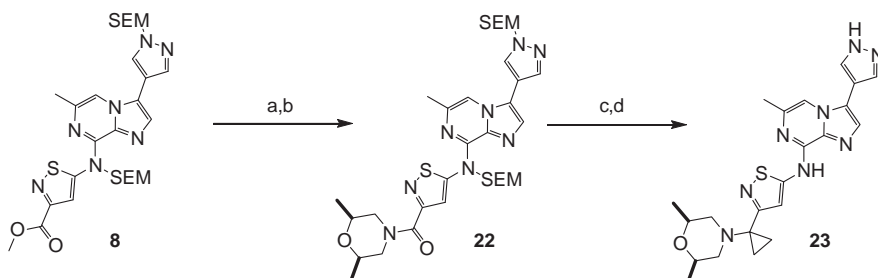
**Figure 1.** Previously disclosed, potent Aurora kinase inhibitors.



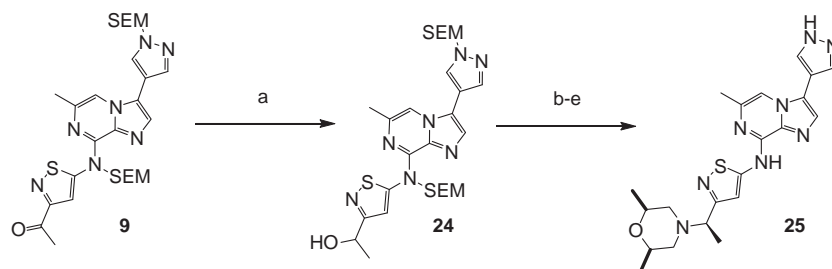
**Scheme 1.** Reagents and conditions: (a) NaH, methyl 5-aminoisothiazole-3-carboxylate, DMSO, rt, 85%; (b) NaBH<sub>4</sub>, CaCl<sub>2</sub>, EtOH/THF, 90%; (c) MsCl, DIEA, THF, 95%; (d) amine, DIEA, NaI, DMF, 60 °C; (e) 4 N HCl dioxane in THF.



**Scheme 2.** Reagents and conditions: (a) SEMCl, Cs<sub>2</sub>CO<sub>3</sub>, DMF, rt, 70%; (b) RMgX, or DMHA-HCl/LiHMDS, or DIBAL, THF, -78 °C; (c) NaBH<sub>4</sub>, CaCl<sub>2</sub>, EtOH/THF, 90%; (d) MsCl, DIEA, THF, 95%; (e) amine, DIEA, NaI, DMF, 60 °C; (f) 4 N HCl dioxane in THF; (g) Me<sub>3</sub>S<sup>+</sup>I<sup>-</sup>/NaH, DMSO, rt, 80%; (h) NaOR', DMF, -10 °C to rt.

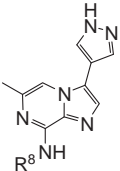


**Scheme 3.** Reagents and conditions: (a) LiOH, THF/MeOH/H<sub>2</sub>O (4:1:1), 99%; (b) cis-2,6-dimethylmorpholine, HATU, DIEA, DMF, 80%; (c) TiCl<sub>4</sub>-Mg-DCM, THF, 0 °C to rt; (d) 4 N HCl dioxane in THF, 15% for two steps.



**Scheme 4.** Reagents and conditions: (a) (+)-DIP-Cl™, THF,  $-40\text{ }^{\circ}\text{C}$ , 78%; (b)  $\text{Ms}_2\text{O}$ , DIEA, THF, rt, quantitative; (c) cis-2,6-dimethylmorpholine, DIEA, THF,  $75\text{ }^{\circ}\text{C}$ , 70%; (d) 4 N HCl dioxane in THF; (e) SFC AS-H enrichment.

**Table 1**  
Data for imidazo[1,2-*a*]pyrazines **2**, **3** and **7a–b**



Compd	R <sup>8</sup>	phos-HH3 EC <sub>50</sub> <sup>a</sup> (nM)	LCK IC <sub>50</sub> <sup>a</sup> (nM)	Rat AUC <sup>b</sup> (μM h)
<b>2</b>		250	568	0
<b>3</b>		24	≤1	0
<b>7a</b>		117	384	3.3
<b>7b</b>		14	45	0.5

<sup>a</sup> All compounds inhibit Aurora A  $\leq 4$  nM and Aurora B  $\leq 13$  nM. Assay conditions listed in Ref. 7.

<sup>b</sup> AUC<sub>0–6 h</sub> (10 mg/kg, po).

N-deethylation of the aminoalcohol side chain. Herein, we describe the discovery of a more kinase selective, orally bioavailable imidazo[1,2-*a*]pyrazine-based Aurora A/B kinase inhibitor that demonstrates anti-tumor activity in a human tumor xenograft mouse model.

The Aurora kinase inhibitors discussed in this work were prepared as shown in Schemes 1–4. Sulfone **4** was prepared in six steps from readily available 3,5-dibromopyrazine.<sup>7</sup> Conversion of sulfone **4** to ester **5** was accomplished in good yield using methyl 5-aminoisothiazole-3-carboxylate<sup>8</sup> and sodium hydride (Scheme 1). Subsequent reduction of ester **5** with  $\text{NaBH}_4/\text{CaCl}_2$  afforded the alcohol **6** which was converted to the corresponding mesylate. Side chain introduction was attained by mild heating of the mesylate in the presence of various amines. Acidic SEM-deprotection afforded compounds **7a–p**.

Functionalization of the aminoisothiazole benzylic position was achieved by first SEM-protecting the 8-position NH group of compound **5** (SEMCl,  $\text{Cs}_2\text{CO}_3$ , Scheme 2). Direct conversion of di-SEM protected ester **8** to the corresponding ketones **9–11** was possible

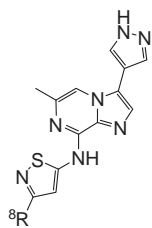
by cryogenic addition of Grignard reagents. On larger scale, more reproducible results were obtained by using the Weinreb amide<sup>11</sup> **13** giving ketones **9–11** with very high purity. DIBAL reduction of the ester **8** afforded aldehyde **12**, which in turn was converted to epoxide **14** using the Johnson–Corey–Chaykovsky reaction.<sup>12</sup> Regioselective epoxide ring opening afforded alkoxy alcohols **15–16**. All alcohol intermediates were converted to final products **17–21** using an analogous sequence as described for compounds in Scheme 1.

The synthesis of cyclopropyl analog **23** commenced with saponification of ester **8** followed by HATU-mediated coupling providing amide **22** in high yield (Scheme 3). Treatment of amide **22** with  $\text{TiCl}_4/\text{Mg}/\text{DCM}$  introduced the cyclopropyl moiety.<sup>13</sup> Acidic global SEM-deprotection afforded the desired cyclopropyl analog **23**.

All chiral compounds were first prepared as racemic mixtures. The promising profile of compound **25** prompted an evaluation of each enantiomer and ultimately led to the development of a scalable asymmetric synthesis. It was envisioned that the key alcohol intermediate **24** could be obtained by asymmetric reduction of prochiral ketone **9** (Scheme 4). To that end, the (+)-DIP-Chloride™ reduction of ketone **9** provided alcohol<sup>14a</sup> **24** with good asymmetric induction (92–94% ee) and in good chemical yield (78%).<sup>14b</sup> Conversion of the enantiomerically enriched alcohol **24** to the desired inhibitor **25** (90–92% ee) was achieved in three steps. Final preparative supercritical-fluid chromatography (SFC) was used to enrich the enantiomeric purity of inhibitor **25** (>99.4% ee).<sup>15</sup>

Previously we disclosed that 8-position basic-functionality improved the physicochemical properties of the imidazo[1,2-*a*]pyrazine series and, in some instances, improved cell-based activity.<sup>8</sup> For example, inhibitor **3** showed excellent cell potency relative to inhibitor **2**, but lacked oral bioavailability (Table 1). Closely related morpholine and piperidine analogs (**7a** and **7b**, respectively) were found to have improved oral exposure in rat relative to compound **3**. Furthermore, both compounds **7a** and **7b** had good cell activity and showed better LCK selectivity (LCK IC<sub>50</sub> = 384 nM and 45 nM, respectively) than inhibitor **3** (LCK IC<sub>50</sub>  $\leq 1$  nM). The attractive profile of morpholine analog **7a** encouraged further SAR exploration.

A series of morpholine and piperazine inhibitors was designed to evaluate the effect of compound lipophilicity and nitrogen basicity on cell potency. Promising compounds were assessed for oral exposure in rat, kinase cross-reactivity and in vitro DMPK properties. Unlike inhibitor **3**, compounds bearing substituted piperazines (analog **7c–j**, Table 2) all displayed moderate to poor cell-based activity. Similarly, morpholine analogs bearing polar functionality (e.g., hydroxymethyl analog **7k**) displayed poor cell potency, while analogs bearing lipophilic alkyl groups (analog **7l–p**) gave compounds with good cell potency. The cis-2,6-dimethylmorpholine analog **7m** showed a modest improvement in cell activity, retained modest LCK selectivity (IC<sub>50</sub> = 420 nM) and had good oral rat exposure. Poor oral mouse pharmacokinetics (50 mg/kg, AUC = 0.8 μM h) limited the potential of compound **7m**.

**Table 2**  
Data for imidazo[1,2-*a*]pyrazines **7c–p**

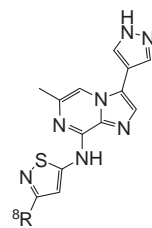
Compd	R <sup>8</sup>	Phos-HH3 <sup>a</sup> EC <sub>50</sub> (nM)	Rat AUC <sup>c</sup> (μM h)
<b>7c</b>		412	nd <sup>b</sup>
<b>7d</b>		561	0.38
<b>7e</b>		>1000	nd <sup>b</sup>
<b>7f</b>		>500	nd <sup>b</sup>
<b>7g</b>		>1000	nd <sup>b</sup>
<b>7h</b>		>1000	nd <sup>b</sup>
<b>7i</b>		>1000	0
<b>7j</b>		>1000	nd <sup>b</sup>
<b>7k</b>		>1000	nd <sup>b</sup>
<b>7l</b>		197	0.4
<b>7m</b>		82	7.3
<b>7n</b>		267	0.4
<b>7o</b>		256	3.9
<b>7p</b>		250	nd <sup>b</sup>

<sup>a</sup> All compounds inhibit Aurora A ≤ 4 nM and Aurora B ≤ 13 nM. Assay conditions listed in Ref. 7.

<sup>b</sup> Not determined.

<sup>c</sup> AUC<sub>0–6 h</sub> (10 mg/kg, po).

Most substitution at the isothiazole benzylic position was tolerated (Table 3). Very good enzyme potency was observed for inhibitors with small alkyl (e.g., –CH<sub>3</sub> **16** and –CH<sub>2</sub>CH<sub>3</sub> **17**), ether moieties (e.g., –CH<sub>2</sub>OCH<sub>3</sub> **19** and –CH<sub>2</sub>OCH<sub>2</sub>CH<sub>3</sub> **20**) or larger heteroaromatics (e.g., 2-pyridyl **18**). Disubstitution of the benzylic position was not tolerated (e.g., cyclopropyl analog **23**). Additional substitution on the morpholine ring was also tolerated (e.g., 2,2-dimethylmorpholine **26** and cis-2,6-dimethylmorpholine **27**).

**Table 3**  
Data for imidazo[1,2-*a*]pyrazines **16–29**

Compd	R <sup>8</sup>	Phos-HH3 <sup>a</sup> EC <sub>50</sub> (nM)	Rat AUC <sup>c</sup> (μM h)
<b>16<sup>d</sup></b>		74	1.1
<b>17<sup>d</sup></b>		49	0.5
<b>18<sup>d</sup></b>		104	0.4
<b>19<sup>d</sup></b>		83	2.3
<b>20<sup>d</sup></b>		281	nd <sup>b</sup>
<b>23<sup>e</sup></b>		733	0.3
<b>25</b>		28	4.6
<b>26<sup>d</sup></b>		71	1.3
<b>27<sup>d</sup></b>		55	8.0
<b>28</b>		217	1.1

Assay conditions listed in Ref. 7.

<sup>a</sup> All compounds inhibit Aurora A ≤ 4 nM and Aurora B ≤ 13 nM, except **28**.

<sup>b</sup> Not determined.

<sup>c</sup> AUC<sub>0–6 h</sub> (10 mg/kg, po).

<sup>d</sup> Racemic.

<sup>e</sup> Compound **23** (Aur A/B IC<sub>50</sub> = 45/50 nM).

**Table 4**  
Selected kinase inhibition profile of Aurora inhibitor **25** and **3**

Kinase	<b>25</b> <sup>a</sup> IC <sub>50</sub> (nM)	<b>3</b> IC <sub>50</sub> (nM)
Aurora A	≤4	≤4
Aurora B	≤13	≤13
LCK	510	≤1
CHK1	140	13
RSK2	330	180
VEGFR2	710	1
IRAK4	1800	37

<sup>a</sup> IC<sub>50</sub>s > 10 μM for Akt1, Camk4, Cdk2, CSNK1d, EGFR, Erk2, EGFR, IKKb, Jak2, cMet, PKCα, PLK3, Rock2 and TSSK2.

Single enantiomer **25** showed good cell-based potency, almost 10-fold better than opposite enantiomer **28**.

Among morpholine derivatives, compound **25** was found to have the most interesting profile and was further evaluated. Compound **25** displayed a phenotype consistent with Aurora A/B kinase inhibi-

**Table 5**  
In vivo pharmacokinetic parameters of Aurora inhibitor **25**

Species	Dose (mg/kg)	AUC <sub>0–∞</sub> (μM h)	Cl (mL/min/kg)	T <sub>1/2</sub> (h)	V <sub>dss</sub> (L/kg)	%F
Rat	10 iv <sup>a</sup>	38.8	10	5.0	1.6	—
Rat	30 po <sup>a</sup>	57.7	—	—	—	72
Mouse	3 iv <sup>b</sup>	5.6	20	3.9	1.5	—
Mouse	50 po <sup>b</sup>	86.4	—	—	—	92
Dog	1 iv <sup>b</sup>	3.4	12	4.8	12	—
Dog	10 po <sup>b</sup>	2.2	—	—	—	50

<sup>a</sup> 0.1% MC.

<sup>b</sup> 20% HPBCD.

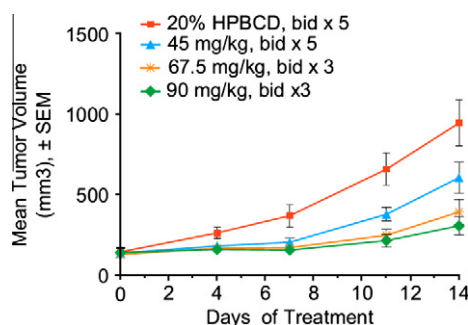


**Figure 2.** In vivo efficacy of inhibitor **25** in A2780 ovarian tumor xenograft.<sup>17</sup>

tion as it decreased phosphorylation of phos-HH3 and induced >4 N DNA content. Moreover, compound **25** displayed potent inhibition of cell growth and survival (EC<sub>50</sub> = 19 and 20 nM, respectively). The off-target kinase inhibition profile of compound **25** was considerably better than compound **3** (Table 4). The inhibitor **25** showed good oral bioavailability in rat, mouse and dog (Table 5) and was chosen to be evaluated in vivo.<sup>16</sup>

The anti-tumor activity of inhibitor **25** was assessed in mice bearing established A2780 ovarian tumor xenografts. Mice were dosed orally at the maximally tolerated dose for 3 or 5 consecutive days: 45 mg/kg b.i.d. × 5 and 90 mg/kg b.i.d. × 3 and 67.5 mg/kg b.i.d. × 3. All three treatments demonstrated dose dependent tumor growth inhibition (TGI), with the best efficacy achieved with 90 mg/kg b.i.d. × 3 (79% TGI, *p* < 0.05). Oral dosing at 45 mg/kg b.i.d. × 5 resulted in 41% TGI (*p* < 0.05) and 67.5 mg/kg b.i.d. × 3 led to 67% TGI (*p* < 0.05) (Fig. 2).

In conclusion, we have discovered a novel and potent imidazo[1,2-*a*]pyrazine-based Aurora kinase inhibitor **25** that shows dose dependent anti-tumor activity in human tumor xenograft model. Compound **25** is orally active and also displays improved off-target kinase inhibition relative to previously reported inhibitors from this series.

## Acknowledgments

We would like to thank Drs. John Piwinski, Paul Kirschmeier, Dan Hicklin and W. Robert Bishop for support of this work. We also would like to thank Lisa H. Peterson, Rachel E. Giessert and Dr. Matthew E. Voss (AMRI) for their contributions to this work. We also would like to thank Michael Starks and Jason Hill for development of chiral SFC methods that were essential for the successful completion of this program.

## References and notes

- (a) Andrews, P. D. *Oncogene* **2005**, *24*, 5005; (b) Pollard, J. R.; Mortimore, M. J. *Med. Chem.* **2009**, *52*, 2629; (c) Carpinelli, P.; Moll, J. *Expert Opin. Ther. Targets* **2008**, *12*, 69.
- Ikezoe, T.; Yang, J.; Nishioka, C.; Tasaka, T.; Taniguchi, A.; Kuwayama, Y.; Komatsu, N.; Bandobashi, K.; Togitani, K.; Koeffler, H. P.; Taguchi, H. *Mol. Cancer Ther.* **2007**, *6*, 1851.
- (a) Dar, A. A.; Zaika, A.; Piazuolo, M. B.; Correa, P.; Koyama, T.; Belkhir, A.; Washington, K.; Castells, A.; Pera, M.; El-Rifai, W. *Cancer* **2008**, *112*, 1688; (b) Wang, X. X.; Liu, R.; Jin, S. Q.; Fan, F. Y.; Zhan, Q. M. *Cell Res.* **2006**, *16*, 356; (c) Ullisse, S.; Delcros, J. G.; Baldini, E.; Toller, M.; Curcio, F.; Giacomelli, L.; Prigent, C.; Ambesi-Impimbato, F. S.; D'Armiento, M.; Arlot-Bonnemains, Y. *Int. J. Cancer* **2006**, *119*, 275.
- (a) Cheung, C. H.; Coumar, M. S.; Hsieh, H. P.; Chang, J. Y.; Coumar, M. S.; Cheung, C. H.; Chang, J. Y.; Hsieh, H. P. *Expert Opin. Invest. Drugs* **2009**, *18*, 379; (b) Perez Fidalgo, J. A.; Roda, D.; Rosello, S.; Rodriguez-Braun, E.; Cervantes, A. *Clin. Transl. Oncol.* **2009**, *11*, 787.
- (a) Tanaka, E.; Hashimoto, Y.; Ito, T.; Okumura, T.; Kan, T.; Watanabe, G.; Imamura, M.; Inazawa, J.; Shimada, Y. *Clin. Cancer Res.* **2005**, *11*, 1827; (b) Kurai, M.; Shiozawa, T.; Shih, H. C.; Miyamoto, T.; Feng, Y. Z.; Kashima, H.; Suzuki, A.; Konishi, I. *Hum. Pathol.* **2005**, *36*, 1281.
- Coumar, M. S.; Cheung, C. H.; Chang, J. Y.; Hsieh, H. P. *Expert Opin. Ther. Patents* **2009**, *19*, 321.
- Belanger, D. B.; Curran, P. J.; Hruza, A.; Voigt, J.; Meng, Z.; Mandal, A. K.; Siddiqui, M. A.; Basso, A. D.; Gray, K. *Bioorg. Med. Chem. Lett.* **2010**, *20*, 5170.
- Yu, T.; Tagat, J. R.; Kerekes, A. D.; Doll, R. J.; Zhang, Y.; Xiao, Y.; Esposito, S.; Belanger, D. B.; Curran, P. J.; Mandal, A. K.; Siddiqui, M. A.; Shih, N.-Y.; Basso, A. D.; Liu, M.; Gray, K.; Tevar, S.; Jones, J.; Lee, S.; Liang, L.; Ponery, S.; Smith, E. B.; Hruza, A.; Voigt, J.; Ramanathan, L.; Prosise, W.; Hu, M. *ACS Med. Chem. Lett.* **2010**, *1*, 214.
- Basso A. D.; Liu M.; Gray, K.; Tevar, S.; Lee, S.; Liang, L.; Ponery, A.; Smith, E. B.; Yu, T.; Monsma, F.; Hicklin, D.; Kirschmeier, P. *Int. J. Cancer*, submitted for publication.
- Src family inhibition by Sprycel® (Dasatinib) causes mild-to-moderate dose limiting toxicities: Hochhaus, A. *Expert Rev. Anticancer Ther.* **2007**, *7*, 1529.
- Williams, J. M.; Jobson, R. B.; Yasuda, N.; Marchesini, G.; Dolling, U.-H.; Grabowski, E. J. J. *Tetrahedron Lett.* **1995**, *36*, 5461.
- Johnson, A. W.; LaCount, R. B. *J. Am. Chem. Soc.* **1961**, *83*, 417.
- Lin, K.-W.; Yan, S.; Hsieh, I. L.; Yan, T.-H. *Org. Lett.* **2006**, *8*, 2265.
- (a) The absolute configuration of alcohol **24** was not determined.; (b) Brown, H. C.; Chandrasekharan, J.; Ramachandran, P. V. *J. Am. Chem. Soc.* **1988**, *110*, 1539.
- Preparative SFC was performed on a Thar SuperPure SFC-350 instrument and a ChiralPak AS-H column 50 × 250 mm with 25% isopropanol/0.2% diethylamine as eluent (flow rate = 250 g/min; back pressure = 225 bar; concentration = 16 mg/mL). The absolute configuration of the amine **25** was determined by X-ray crystal structural analysis.
- Compound **25** was designed for oral dosing, but equilibrium solubility studies showed that it was suitable for dosing by intravenous injection (solubility in 20 mM Acetate buffer, pH4 = 4.66 mg/mL).
- Xenograft studies.* For solid tumor xenograft models, nu/nu mice (5–7 weeks of age) were injected subcutaneously with  $5 \times 10^6$  A2780 cells/mouse. When tumor cells reached approximately 200 mm<sup>3</sup>, mice were randomly grouped into treatment groups (*n* = 10). Tumor volumes and body weights were measured twice a week throughout the study using calipers and calculated by the formula (width × length × height) × 6/π. Statistically significant differences were determined by the multiple comparison one way ANOVA (Turkey's test) at the 95% confidence level using GraphPad Prism. All animal studies were carried out in accordance with institutional guidelines and the NIH Guide for the Care and Use of Laboratory Animals.